Performance of a picosecond x-ray delay line unit at 8.39 keV

Wojciech Roseker,[1,*] Hermann Franz,[1] Horst Schulte-Schrepping,[1] Anita Ehnes,[1] Olaf Leupold,[1] Federico Zontone,[2] Aymeric Robert,[3] and Gerhard Grübel[1]

[1]*Hamburger Synchrotronstrahlungslabor am Deutschen Elektronen Synchrotron (DESY), Notkestrasse 85, D-22603 Hamburg, Germany*

[2]*European Synchrotron Radiation Facility, 6 rue Jules Horowitz, BP 220, 38043 Grenoble Cedex 09, France*

[3]*SLAC National Accelerator Laboratory, 2575 Sand Hill Road, Menlo Park, California 94025, USA*

**Corresponding author: wojciech.roseker@desy.de*

Received March 9, 2009; accepted April 16, 2009;
posted May 7, 2009 (Doc. ID 108528); published June 2, 2009

A prototype device capable of splitting an x-ray pulse into two adjustable fractions, delaying one of them with the aim to perform x-ray photon correlation spectroscopy and pump–probe type studies, was designed, manufactured, and tested. The device utilizes eight perfect silicon crystals in vertical 90° scattering geometry. Its performance has been verified with 8.39 keV synchrotron radiation. The measured throughput of the device with a Si(333) premonochromator at 8.39 keV under ambient conditions is 0.6%. Time delays up to 2.62 ns have been achieved, detected with a time resolution of 16.7 ps. © 2009 Optical Society of America

OCIS codes: 340.0340, 340.6720, 140.2600, 320.7100.

Forthcoming x-ray free electron laser (XFEL) sources will produce ultrashort, coherent, and very intense x-ray pulses enabling one to probe ultrafast dynamics in condensed matter on the subnanometer-length scale. However, the time structure of XFEL machines compromises the accessible time windows for some experimental techniques. In x-ray photon correlation spectroscopy (XPCS) [1], or x-ray pump/x-ray probe experiments, the shortest time scale that can be traced is set by the pulse duration and the minimum bunch spacing of the source. The time structure of the European XFEL facility in Hamburg, Germany [2], consists of 100 fs short single pulses separated by 200 ns arranged into bunch trains of 3000 pulses arriving with a repetition rate of 10 Hz. The Linac Coherent Light Source (LCLS) in Stanford, California [3], will provide 100 fs short x-ray pulses with a repetition rate of 120 Hz. Studying dynamics with XPCS or an x-ray pump/x-ray probe technique at time scales shorter than 200 ns at the European XFEL or 8.3 ms at LCLS will be experimentally not feasible. The availability of photon time delay lines will allow one to adapt the time structure of the source to the needs of the experiment. In this way time scales close to the pulse length can be accessed independently of the minimum bunch spacing. Photon delay lines are known for visible radiation down to the soft x-rays spectral range [4]. Equivalent devices for hard x rays have been discussed for many years [2,3,5,6], but up to now only one attempt to delay x-ray pulses at high photon energies has been reported [7].

In this Letter, we report on the performance of the to our knowledge first hard x-ray delay line unit, which is continuously tunable between 0 and 2.62 ns with a (detector limited) time resolution of 16.7 ps. The device opens up new possibilities for fast time domain x-ray diffraction [2,3,8], and pump–probe experiments at XFEL sources.

The concept of the delay line is based on splitting an x-ray pulse into two fractions, delaying one of them and recombining both pulses on a common path. A scheme of this concept is shown in Fig. 1. The device consists of eight single crystals arranged in 90° vertical-scattering geometry. The incoming pulse is split by a first crystal (BS) into two, that propagate along two unequal rectangular paths. For one part of the pulse the optical path is defined by Bragg crystal reflectors BR-I, BR-II, and BR-III (called upper branch). The second part of the beam is guided via the BR-IV, BR-V, and BR-VI crystals, (lower branch). Both beams are recombined with the help of the beam mixer (BM). The beam is reflected inside the delay line by using perfect Si(511) crystals oriented in symmetric Bragg geometry (called Bragg crystals) [9]. The peak reflectivity and the angular acceptance of a Si(511) crystal at 8.39 keV is 0.89 and 8.6 μrad, respectively [10]. The beam splitting and mixing is accomplished by wedge-shaped Si(511) perfect crystals oriented in Laue geometry (called Laue crystals). Owing to the Pendellösung effect [9], which is a unique diffraction phenomena for Laue geometry, the

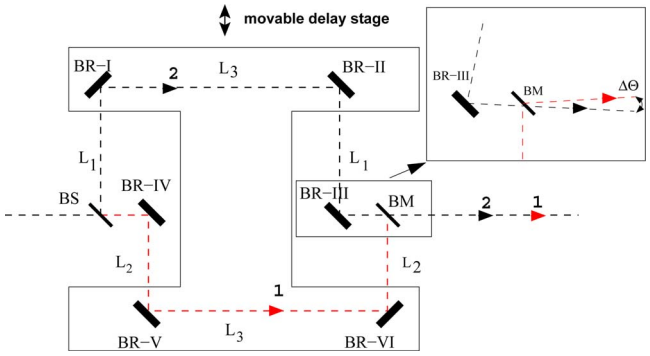

Fig. 1. (Color online) Basic concept of the x-ray delay line. Eight optical components arranged in 90° scattering scheme. BR-I, BR-II, BR-III, BR-IV, BR-V, BR-VI, Bragg reflectors; BS, beam splitter, BM, beam mixer. L_1, L_2, L_3, path lengths inside the delay line. Inset, angular mismatch $\Delta\Theta$ between the two exit beam paths for Laue–Bragg optics.

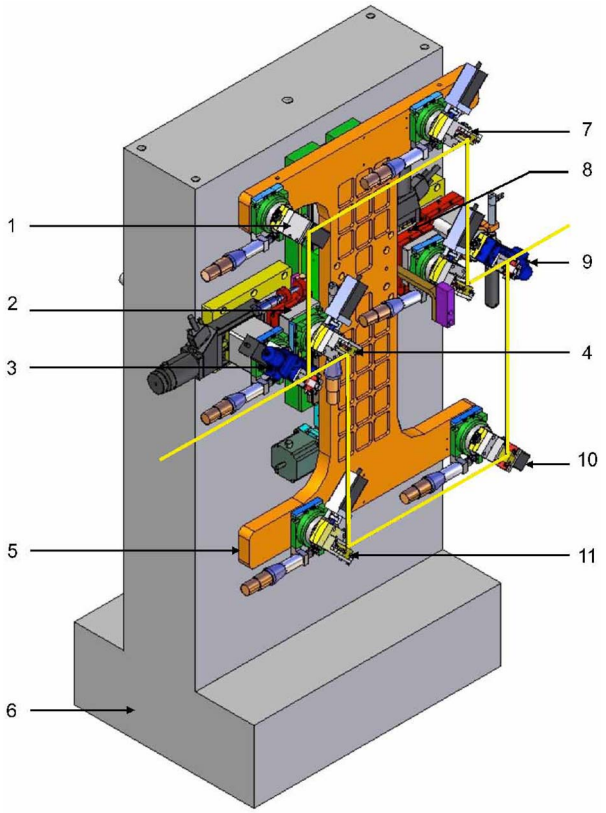

Fig. 2. (Color online) Three-dimensional model of the delay line. 1, 2, 4, 7, 10, 11, Bragg reflector stages; 3, beam splitter stage; 9, beam mixer stage; 5, aluminum plate; 6, granite support. The x-ray beam path is denoted by a gray (yellow online) line.

intensity ratio of the two outgoing x-ray pulses (i.e., the main pulse and its delayed replica) can be easily controlled and selected appropriately for pump–probe and XPCS experiments. For XPCS studies a splitting ratio of 1:1 is desirable, which can be achieved by using a 27 μm thin Laue crystal.

By combining Bragg and Laue optics in the delay line one modifies the scattering paths of the x-ray beam inside the device leading to a deviation from the perfect 90° scattering geometry. This causes the pulses delayed by the upper and lower branches to exit the delay line with an angular mismatch $\Delta\Theta$, as shown in the inset of Fig. 1. The mismatch at an energy of 8.39 keV and Si(511) optics is 54.5 μrad. This mismatch can be remedied by using a Bragg beam splitter and Bragg beam mixer, by temperature tuning of the Laue optics, applying alternative scheme for the arrangement of the delay branches, or, as applied here, by appropriately tilting the crystals of the upper and lower branch.

The delay time between the two split pulses is given by

$$\tau_c = \Delta L/c. \quad (1)$$

where ΔL is the path length difference between the upper and lower branches and c is the speed of light. As illustrated in Fig. 1 the path lengths difference ΔL is $2\times(L_1-L_2)$. The delay τ_c can be simply changed by varying ΔL. This is achieved by a simultaneous vertical movement of the BR-I, BR-II, BR-V, and BR-VI crystals, mounted on a single translation unit. The other four crystals (i.e., BS, BR-III, BR-IV, BM) are fixed to the rigid granite support. This is illustrated in Fig. 2. The translation unit (5) allows for a 300 mm movement of the BR-I(1), BR-II(7), BR-V(10), and BR-VI(11) crystals in the vertical plane, providing a maximum accessible delay time of 2.66 ns in the current setup. When $L_1=L_2$ the path length difference ΔL is 0 and consequently τ_c as well. Accessing $\tau_c=0$ is of particular interest, since it allows one to calibrate the delay line independently of the mounting precision of the employed mechanics. To maintain the reflection conditions, the experimental setup, shown in Fig. 2, was equipped with very high precision mechanics. High (microradians) angular resolution and stability was achieved by mounting piezo actuators on every crystal stage. To align the beam to the scattering plane and compensate for the angular mismatch of the exit beams, all crystals were placed on tilt stages. The translation unit (5) was equipped with a microstepper, which allows one to set the delay time with a delay time step of 7 fs.

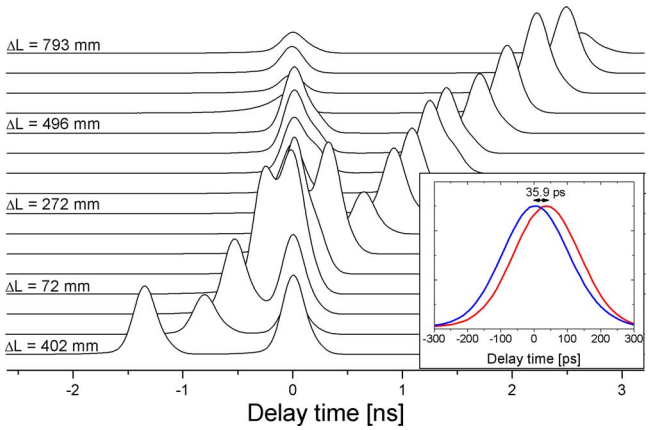

Fig. 3. (Color online) Time patterns measured as a function of path length difference ΔL between the two branches of the delay line. Inset, time patterns recorded when either the upper [gray curve (red online)] or the lower [black curve (blue online)] branch of the delay line was blocked.

The results, which we present here, were obtained at the beam line ID10C(Troïka) at the European Synchrotron Radiation Facility (ESRF). Preliminary performance tests of the delay line were carried out at the beam lines C and W1 of the DORIS III storage ring at HASYLAB/DESY. The performance of the delay unit optics has been verified with 8.39 keV x rays. The overall throughput of the delay line obtained with a Si(333) premonochromator and a photon beam divergence of 17 μrad was measured by comparing incident and exit intensities, yielding a measured throughput $T_M=0.6\%$. The calculated performance (based on ray tracing [11] and including absorption) gives a comparable value $T_{\mathrm{CALC}}=0.62\%$, indicating a very good performance of the delay line optics.

Figure 3 shows a graph of pulse patterns recorded during four-bunch mode operation of the ESRF storage ring. In this mode 125-ps-long electron bunches in the storage ring are separated in time by 704 ns. The time interval between detected photons and the

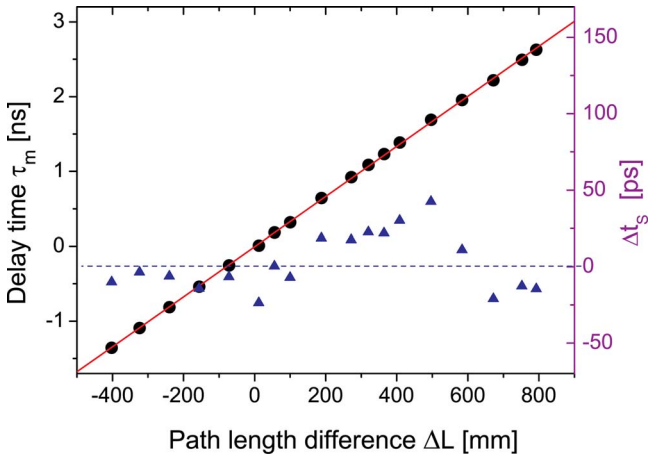

Fig. 4. (Color online) Left axis, measured delay time τ_m versus path-length difference ΔL. Negative values of τ_m and ΔL denote inversed photon pulse arrival times. The solid line is the linear fit to the data. Right axis, difference between the set and measured delay time Δt_s.

synchrotron bunch clock signal was measured in a stroboscopic manner [12] at different settings (i.e., path lengths differences ΔL) of the delay line. Each measured time pattern was normalized to the number of monitor counts, measured upstream the delay line. For clarity reasons the pulse delayed by the lower branch was offset to $t=0$. The peak shape and the intensity varies for all time-delay patterns. This is due to change of absorption in air and nonideal alignment procedure of the delay line. Delay times were extracted by fitting asymmetric Gaussian functions [13] to each time pattern. A maximum delay time of 2.626 ± 0.003 ns was achieved in the experiment. The minimum delay time achievable by the setup is not limited by the pulse length. The analysis showed that pulses separated by more than about 36 ps can be easily resolved (as shown in the inset of Fig. 3). Figure 4 shows a plot of the measured delay time as a function of the path length difference ΔL. The solid line is a least-squares fit to the data, which yields a slope of $3.35\pm0.01\times10^{-3}$ ns/mm and an offset of -4.3 ± 3.2 ps. The delay time error $\Delta t_s=\tau_m-\Delta L/c$ was extracted for every data point, and the results are shown in Fig. 4 by triangles. The mean error is 16.7 ps. Since the uncertainty of setting ΔL is only 0.5 μm (i.e., 7 fs), the main contribution to the measured error is the time resolution of the detection system (i.e., detector and bunch clock electronics). The achieved time resolution of 16.7 ps thus does not represent an intrinsic property of the delay line. Much better time resolutions could be achieved with a higher resolution detection system. The linearity between the path length difference ΔL and the measured delay time τ_m shows that the delay line can be operated without the need for higher-order correction terms when setting the path-length difference.

In conclusion, we have developed a hard x-ray delay line unit, a unique tool for conducting ultrafast XPCS and x-ray pump/x-ray probe studies. The device was commissioned at 8.39 keV. The throughput of the setup at the aforementioned energy is 0.6%. Delay times up to 2.62 ns have been achieved with a time resolution of 16.7 ps, a value determined by the detection system. The obtained results have shown that the x-ray delay line is operational for first experiments with XFEL radiation.

The authors thank R. Rüffer and T. Deschaux of the European Synchrotron Radiation Facility for providing the fast APD detector. K. Rickers-Appel, W. Caliebe, and L. M. Stadler from HASYLAB are acknowledged for their assistance with the experiments.

References

1. G. Grübel and F. Zontone, J. Alloys Compd. **362**, 3 (2004).
2. http://xfel.desy.de/.
3. http://www-ssrl.slac.stanford.edu/lcls/science.html.
4. R. Mitzner, M. Neeb, T. Noll, N. Pontius, and W. Eberhardt, Proc. SPIE **5920**, 86 (2005).
5. Technical Design Report, Part V, G. Materlik and Th. Tschentscher, eds. (DESY, 2001).
6. http://ssrl.slac.stanford.edu/lcls/cdr/.
7. S. Joksch, W. Graeff, J. Hastings, and D. P. Siddons, Rev. Sci. Instrum. **63**, 1114 (1992).
8. G. Grübel, G. B. Stephenson, C. Gutt, H. Sinn, and Th. Tschentscher, Nucl. Instrum. Methods Phys. Res. B **262**, 357 (2007).
9. B. W. Batterman and H. Cole, Rev. Mod. Phys. **36**, 681 (1964).
10. R. J. Dejus and M. S. del Rio, Proc. SPIE **3152**, 148 (1997).
11. O. Seeck, *HASYLAB Annual Report* (HASYLAB, 2006), pp. 333–336.
12. S. Kishimoto, Rev. Sci. Instrum. **63**, 824 (1992).
13. T. Kato, S. Omachi, and H. Aso, Lect. Notes Comput. Sci. **2396**, 405 (2002).